mL) at −60 °C and vacuum dried at 0 °C. Yield: 0.13 g, 40%. Anal. Calcd for $C_{11}H_{18}BrCr$: C, 46.86; H, 6.43; Br, 28.35. Found: C, 42.89; H, 5.92; Br, 26.68.

Determination of K_{eq} for the Equilibrium between 2 and 3. The value of K_{eq} for the equilibrium $[Cp^*CrMeCl]_2 \rightleftarrows 2[Cp^*CrMeCl]$ was estimated using the concentration dependence of the intensity of the characteristic EPR signal of **3** in Figure 2. For a simple dimer–monomer equilibrium, where $K_{eq} = [\mathbf{3}]^2/[\mathbf{2}]$ and $[Cr]_{total} = [\mathbf{3}] + 2[\mathbf{2}]$, it can be shown that solving for [**3**] and taking the real root gives the expression

$$[\mathbf{3}] = (1/4)K_{eq}(\{(8[Cr]_{total} + 1)/K_{eq}\}^{1/2} - 1) \quad (1)$$

Since the EPR signal of **3** is not observed in Figure 2A, this sets the limit that $[\mathbf{3}]/[Cr]_{total} < 0.01$ at $[Cr]_{total} = 8 \times 10^{-2}$ M. A value of $K_{eq} = 1 \times 10^{-6}$ gives $[\mathbf{3}]/[Cr]_{total} = 0.0025$, which is consistent with the absence of the monomer signal in Figure 2A. While **3** appears to have a $S = {}^1/_2$ ground state, the origin of the signal from **2** is not clear, making it difficult to compare quantitatively the two signal intensities. However, if the EPR signal of **2** arises from the thermally populated $S = 2$ state (antiferromagnetic coupling[3b]), then at 205 K for $K_{eq} = 1 \times 10^{-6}$ we calculate the signal intensity ratio, $I(\mathbf{3})/I(S = 2 \text{ of } \mathbf{2})$, to be 1/11, 1/3, and 3/1 for parts A, C, and D of Figure 2, respectively; this is the correct trend, with only the Figure 2D ratio appearing to be too small.

Acknowledgment. We are grateful to Robert Ditchfield and Russell Hughes for valuable discussions and thank Russell Hughes for the use of his glovebox. We thank one reviewer for drawing our attention to overlap between the chloride p_y and chromium d_{xy} orbitals in **3** and another for pointing out the relationship between monomer and total metal concentrations for a dimer–monomer equilibrium. The EPR spectrometer was purchased in part with funds from the National Science Foundation (Grant CHE 8701406) and the Dreyfus Foundation.

Contribution from the Departments of Chemistry and Physics, Rutgers University, New Brunswick, New Jersey 08903

Ligand Isomerism and Stacking in Square Planar Platinum(II) Complexes

M. J. Coyer,[‡] M. Croft,[§] J. Chen,[§] and R. H. Herber*,[‡]

Received September 12, 1991

The structure and bonding in two forms of the bisthiocyanate complex of Pt(II), $Pt[(bpy)(X)_2]$ (where bpy is 2,2′-bipyridyl and X is the pseudohalide), have been studied by solution and solid-state NMR, FTIR, and EXAFS spectroscopies. The yellow complex, which is soluble in a variety of organic solvents, contains two cis S-bonded SCN ligands and is the kinetically favored form. On heating, either in solution or as a solid, this complex transforms to a red insoluble complex, in which the SCN ligands have "flipped" to become N-bonded and which appears to be the thermodynamically stable form at room temperature. Conversion of the solid does not involve loss of a solvent molecule. EXAFS experiments involving the Pt-L_3 edge show the presence of two Pt–Pt distances in the red solid, one of which is indicative of the formation of stacked square planar Pt moieties, in which the 18-electron rule is satisfied.

The majority of known complexes of Pt(II), a d^8 transition metal, involve Pt sp^2d hybridization, giving rise to a square planar coordination of the ligands around the metal center. Such complexes display a rich (and challenging) set of chemical and physical properties, including various types of isomerism,[1] polychromism,[2] optical properties,[3] and a tendency to form chain-type polymers with anisotropic transport properties.[4] In addition, their importance as antineoplastic chemotherapeutic agents[5] have made these complexes the subject of intense study in recent years.

In particular, the thiocyanate complexes of Pt(II) have aroused considerable attention because of their unusual chemical and physical properties and have been the subject of several recent reviews.[6,7] The bisthiocyanate complexes of Pt(II), in which two coordination sites are occupied by a bidentate ligand, thus forcing the pseudohalide ligands to occupy cis positions, are of particular interest. Subtle chemical modifications of the bidentate ligand can be used to influence the nature of the pseudohalide bonding and the solvation of the solids, as well as the chemical properties of the product. In his extensive review of "ambidentate ligands", Burmeister[7] points out that there are, in fact, 10 distinguishable modes in which the SCN group can bond to a metal center, including ionic, simple covalent, bridging, linear, and bent bond formation. Of these, the M–SCN (type 13) and M–NCS (type 12) ligations are most fundamental in understanding the interaction between Pt and the "soft" (more easily polarizable, i.e., S) and "hard" (i.e., N) end of the ligand as it exists in a particular complex.

In this context, it was reported some time ago[8] that the bisthiocyanate complex of Pt(bipy) (where bipy is 2,2′-bipyridyl) can exist in two isomeric forms: a yellow complex which is soluble in a variety of (coordinating) solvents and which transforms under relatively mild conditions to a polymeric (red) species, which is insoluble and stable under ordinary conditions. As has been discussed by Kukushkin et al.[8] the two forms have the same stoichiometry, but their chemical and optical properties are distinctly different. This difference has been ascribed to several possible factors, including solvation,[2] polymerization, and ligand isomerization.[8] The latter possibility and its spectroscopic consequences have been discussed in detail by Burmeister,[7a] and an X-ray diffraction study of both S- and N-bonded thiocyanate complexes of palladium (1,1,7,7-tetraethyl)diethylenetriamine salts with tetraphenyl borate anions has been reported by Brock et al.[7b] However, to date (to the best of our knowledge) no single-crystal X-ray diffraction data have been reported which give unambiguous evidence for the ligand "flip" in Pt(II) complexes, which must

‡ Department of Chemistry.
§ Department of Physics.

(1) Engelter, C.; Thornton, D. A. *J. Mol. Struct.* **1977**, *42*, 51; Clark, R. J. H.; Williams, C. S. *Spectrochim. Acta* **1966**, *22*, 1081; Thompson, L. K. *Inorg. Chem.* **1980**, *38*, 117.
(2) Bielli, E.; Gidney, R. D.; Gillard, R. D.; Heaton, B. T. *J. Chem. Soc., Dalton Trans.* **1974**, 2133.
(3) Biedermann, J.; Wallfahrer, M.; Gliemann, G. In *Photochemistry and Photophysics of Coordination Compounds*; Yersin, H., Vogler, A., Eds.; Springer Verlag: Berlin, 1987.
(4) Williams, J. M. *Adv. Inorg. Chem. Radiochem.* **1983**, *25*, 235.
(5) Lippert, B. In *Progress in Inorg. Chem.*; Lippard, S. J., Ed.; Wiley and Sons: New York, 1989; Vol. 37; Lippard, J. J. *Pure Appl. Chem.* **1987**, *59*, 731; Reedijk, J. *Pure Appl. Chem.* **1987**, *59*, 181; Bednarski, P. J.; Ehrensperger, E.; Schoenberger, H.; Burgemeister, T. *Inorg. Chem.* **1991**, *30*, 3015 and references therein; Farrell, N. *Transition Metal Complexes as Drugs and Chemotherapeutic Agents*; Kluver Academic Publishing Co.: Dordrecht, The Netherlands, 1989; p 67; Gill, D. S. In *Platinum Compounds in Cancer Chemotherapy*; Hacker, M. P., Douple, E. B., Krakoff, I. H., Eds.; Martinus Nijhoff Pub. Co.: Boston, 1984.
(6) Burmeister, J. L. *Coord. Chem. Rev.* **1968**, *3*, 225; Basolo, F. *Coord. Chem. Rev.* **1990**, *100*, 47.
(7) (a) Burmeister, J. L. *Coord. Chem. Rev.* **1990**, *105*, 77. (b) Brock, C. P.; Huckaby, J. L.; Attig, T. G. *Acta Crystallogr.* **1984**, *B40*, 595.
(8) Kukushkin, Yu. N.; Vrublevskaya, L. V.; Vlasova, R. A.; Isachkina, T. S.; Postnikova, E. S.; Sheleshkova, N. K. *Zh. Neorg. Khim.* **1985**, *30*, 401; *Russ. J. Inorg. Chem.* (Engl. Transl.) **1985**, *30*, 224.

0020-1669/92/1331-1752$03.00/0

Table I. Summary of IR Data in the CN Stretch Region for $PtLX_2$ (L = 2,2'-bipyridyl, X = SCN)

compound	form	ν_{CN}/cm^{-1} ($\Gamma_{1/2}/cm^{-1}$)[a]	$\nu_{CN}(1)$[b]/cm^{-1} ($\Gamma_{1/2}/cm^{-1}$)	$\nu_{CN}(2)$[c]/cm^{-1} ($\Gamma_{1/2}/cm^{-1}$)
I	$-(SCN)_2$[d]	2130.9_{sym} (5), 2118.6_{asym} (14)		
II	$-(NCS)_2$[e]	2118.4 (14)	2127.2 (12)	2108.2 (24)
	$-(NCS)_2$[f]	2115.9 (16)	2125.9 (11)	2107.0 (23)
	$-(NCS)_2$[g]	2116.5 (15)	2127.1 (11)	2108.4 (22)
	$-(^{15}NCS)_2$[f,h]	2086.4 (15) [2119.2]	2097.7 (11) [2130.6]	2076.5 (23) [2109.1]
	$-(^{15}NCS)_2$[g,h]	2085.1 (23) [2117.8]	2096.7 (20) [2129.6]	2073.8 (38) [2106.4]
	$-(N^{13}CS)_2$[f,i]	2070.4 (15)	2080.1 (12)	2062.7 (20)
mean values	$-(NCS)_2$	2117.1 (17)	2127.5 (13)	2107.7 (25)

[a] $\Gamma_{1/2}$ refers to line width at half-maximum. [b] $\nu_{CN}(1)$ is the highest frequency band in the ν_{CN} stretching region (see text). [c] $\nu_{CN}(2)$ is the lowest frequency band in the ν_{CN} stretching region (see text). [d] Synthesized by diaquothiocyanate metathesis discussed in the text. [e] From I by heating the solid at 100 °C for ~2 h in vacuum or air. [f] From I by heating the DMSO solution, filtration, and slow cooling. [g] From I by heating the NMP solution, filtration, and slow cooling. [h] ^{15}N labeled complex; numbers in brackets are calculated ^{14}N values. [i] ^{13}C labeled complex; numbers in brackets are calculated ^{12}C values.

occur in going from the M–SCN to the M–NCS form. Moreover, the relationship between this flip and the stacking of complexes to give Pt–Pt interactions (and an effective 18-electron configuration around the metal atom) has not been examined in detail.

In the present study, extended X-ray absorption edge measurements (EXAFS) in conjunction with detailed FTIR spectroscopic and solution and solid-state NMR measurements on ^{15}N and ^{13}C isotopically labeled species have been carried out to provide a more detailed description of the differences in the two forms of the bipyridyl complex and to account for the chemical behavior of platinum with respect to the ambidentate SCN ligand.

Experimental Section

(a) Synthesis of the Complexes. (1) Pt[L(SCN)$_2$] [L = 2,2'-Bipyridyl (bpy) and 1,10-Phenanthroline (phen)]. Commercial K_2PtCl_4 (Aldrich) was used without further purification and converted into Pt[L(Cl_2)] by literature methods.[9] A known amount of this product was dissolved in a minimum amount of DMSO with heating, and to this was added twice the stoichiometric amount of $AgClO_4$ in ca. 5 mL of H_2O, yielding immediately a gray precipitate of AgCl and a yellow solution. The solution was stirred at 100 °C for 1 h and filtered through a sintered glass filter to yield a clear yellow solution. To this was added 5 mL of DMSO to avoid precipitation, and the liquid was cooled to 0 °C. An excess of KSCN in distilled water was added dropwise with stirring to the cold solution to afford instantaneously a bright yellow solid. The solid was filtered (M-grade frit) and washed with cold H_2O, EtOH, and Et_2O and dried under vacuum at room temperature. The solid must be maintained at room temperature (or below) to avoid conversion to the red form (vide infra). Yield: ca. 90%. Anal. for Pt(bpy)$(SCN)_2$ found (calcd): C, 30.51 (30.84); H, 1.67 (1.73); N, 11.65 (11.99); S, 13.46 (13.72). The synthesis of the ^{13}C- and ^{15}N-labeled compounds (vide infra) was identical except that the appropriate isotopic sodium thiocyanate (MSD Corp.) was employed in the last step.

(2) Preparation of the "Red" Pt[L(NCS)$_2$] Complexes. The yellow complexes can be converted to the red form either by dissolving the former in DMSO and heating to 150 °C and allowing the solution to cool slowly to room temperature (filtered and washed with EtOH and Et_2O) or by heating the neat solid in air or vacuum. The rate of the latter transformation, which can also be observed for the yellow solid pelleted with KBr, is temperature dependent and is essentially complete in 2 h at $T > 85$ °C.

(b) Infrared Studies. Midrange IR spectra were accumulated for the microcrystalline powder samples using standard KBr pelleting techniques in conjunction with a Mattson Instruments Cygnus 100 spectrometer operated at 2 cm^{-1} resolution. Kel-F grease mulled samples, examined in the CN stretching region, were also obtained to ensure the absence of reaction of the complexes with KBr. Typically, 64 scans were co-added and ratioed to a KBr background. The resultant interferograms were translated into ASCII format and analyzed, using the Spectracalc software[10] to resolve (nearly) overlapping peaks, especially in the CN stretching region near 2100 cm^{-1}.

(c) NMR Studies. (1) Solution Spectra. The ^{13}C NMR data were obtained with natural abundance as well as 99% $S^{13}CN$ enriched samples, using a 200-MHz Varian Model XL spectrometer. Samples (ca. 1 mL) of the title compounds were prepared from saturated solutions of *N*-methylpyrrolidone (NMP) and filtered to remove any solid. The S-bonded Pt complexes were found to be soluble in a variety of aprotic solvents (i.e., DMSO, DMF, and NMP). The latter was used since the yellow complex remained in solution for a sufficient time at room temperature to permit the obtaining of good signal-to-noise ratio spectra, free of interferences from precipitated sample. The data were acquired at room temperature using a 2-s delay time between pulses to allow adequate time for the slow relaxation of the pseudohalide carbon atom. The total acquisition time was 12 h. DMSO-d_6 in a sealed capillary was introduced into the NMR tubes as an internal locking standard and scale reference.

(2) Solid-State Spectra. The ^{13}C MAS NMR spectra of the yellow and red bpy complexes were obtained using a JEOL GSX 270-MHz spectrometer at a transmitter frequency of 67.80 MHz and delay times of 30 (yellow) and 60 (red) s, respectively. Chemical shifts were calibrated indirectly by use of an external sample of adamantane (29.50 ppm relative to TMS as a reference). The ^{15}N MAS NMR measurements were carried out on a 200-MHz Varian Model XL spectrometer using a 7-mm DOTY probe. The ^{15}N chemical shifts were measured at a transmitter frequency of 15.00 MHz referenced with 99% enriched $(^{15}NH_4)_2SO_4$ to zero ppm, with a spinning rate of ca. 3000 Hz. Exploratory experiments afforded appropriate delay times (D_1). Final values chosen were 30 s for Pt–S^{15}N compounds and 60–90 s for the Pt–^{15}NCS compounds, which exhibit characteristically longer relaxation times than the former, on the basis of comparisons of intensities of each species with similar sample quantities and number of transients recorded. The acquisition time was 0.320 s based on a fit of the free induction decay (fid) signal. The time required to obtain acceptable signal-to-noise ratio spectra varied from 5 to 12 h, depending on the sample concentrations and associated delay times.

(d) EXAFS Studies. The EXAFS measurements were carried out in the absorption mode on beam line X18B and X19A at the Brookhaven National Laboratory Light Source and at station C2 at the Cornell High Energy Synchrotron Source. Multiple absorption coefficient scans over a range of 1000 eV above the Pt-L_3 edge were needed to obtain data of sufficient quality to extract significant high-k information on the Pt–Pt interaction (vide infra). A Displex (Air Products Co.) refrigerator was used to effect cooling for the low temperature measurements. Data analysis was performed using a modified version of the University of Washington program.[11]

(e) Gravimetric Studies. The thermal stability of the subject compounds was examined using a Du Pont Model 9900 Thermal Analyzer in the range $30 < T$ °C < 350. Sample weight changes as small as 0.05% are readily detected by this equipment.

Results and Discussion

In the following discussion, the yellow form of Pt[(bpy)$(SCN)_2$] will be identified as compound I, while the red form, Pt-[(bpy)$(NCS)_2$], will be identified as compound II, unless otherwise noted.

(a) Infrared Data. The midrange IR spectra were examined in detail in the CN stretching region, as well as in the region associated with the CS stretch of the N-bonded thiocyanate group,

(9) Rosenblatt, F.; Schleede, A. *Ann. Chemie (Paris)* **1933**, *505*, 51; Morgan, G. T.; Burstall, F. H. *J. Chem. Soc.* **1934**, 965.
(10) Spectracalc (Lab Calc Arithmetic Package): Galactic Industries Corp., Salem, NH., 1990.
(11) University of Washington Program for EXAFS Data Analysis; See also, Kincaid, B. M.; Shulman, R. In *Advances in Inorganic Biochemistry*; Parnall, D. W., Wilkins, R. G., Eds.; Elsevier: New York, 1980; Vol. 2, pp 303–309; Lee, P. A.; Beni, G. *Phys. Rev.* **1977**, *B15*, 2862; Shulman, R. G.; Eisenberger, P.; Teo, B. K.; Kincaid, B. M.; Brown, G. S. *J. Mol. Biol.* **1978**, *124*, 305.

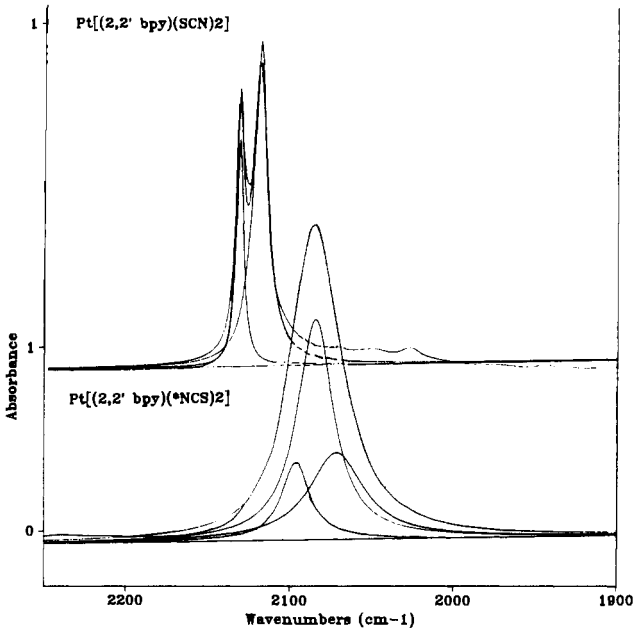

Figure 1. Portion of the IR spectra of I and II in the CN stretching region. The upper trace in each set is the experimental data curve, the lowest trace is that of the (presumed linear) baseline, and the intermediate curves are of the computer generated components. The shift of the bottom spectrum, compound II, relative to the top spectrum, compound I, arises from the ^{15}N label of the thiocyanate ligand.

and the results are summarized in Table I. A typical portion of the spectrum in the CN stretching region is shown in Figure 1. The observed values for I are in reasonable agreement with those reported by Bertini and Sabatini[12] for a number of S-bonded palladium bisthiocyanate complexes, as well as the results of Burmeister and Basolo[13] for Pd(bipy)$(SCN)_2$. The CN stretching frequencies for I are not otherwise remarkable, the symmetric and asymmetric modes, expected to be IR active in C_{2v} point group symmetry, being easily resolved in the spectra.

The appearance of the CN stretching mode region for II is both qualitatively and quantitatively different from that observed for I and is reflected in the lower trace of Figure 1. The gross appearance of the IR band(s) is of a broad singlet, centered at about 2117 cm^{-1}. The change in band shape of the CN stretch in going from M–SCN to M–NCS bonding has been noted by a number of earlier investigators[14-16] and was consistently observed in the present study as a general broadening of the absorption band shape. This broadening can be seen from a comparison of the full width at half-maximum parameter (Γ) summarized in Table I. The use of curve resolution data analysis methods[10] showed that this broad envelope arises from three contributions which overlap sufficiently to give the observed band shape. Attempts to fit the data with only two Lorentzian contributions lead to a consistently poorer value of χ^2 (goodness of fit). IR examination of the ^{15}N and ^{13}C thiocyanate labeled samples of II used in the NMR experiments showed that all three absorbances arise from the SCN group (i.e., are not impurity or ligand modes accidently degenerate with the pseudohalide mode). Reduced mass calculations of the absorbance band centers, assuming no significant coupling of the CN and CS stretches, agree within 0.1 cm^{-1} with the values observed for the unlabeled samples.[17,18] The absorbance

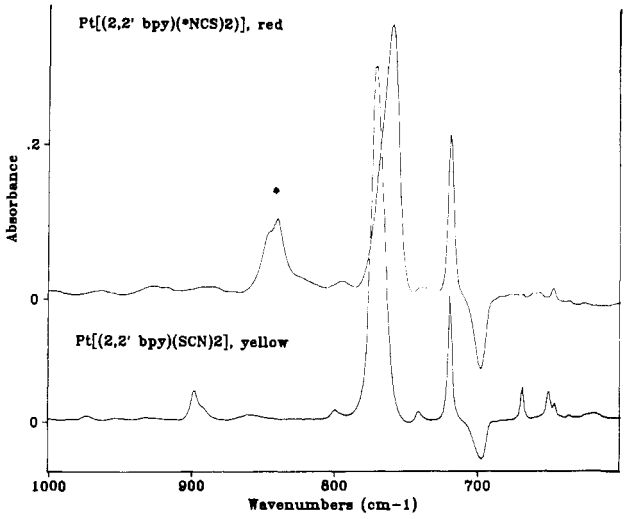

Figure 2. Portion of the IR spectra of I and II in the CS stretching region. The upper trace shows the presence of two absorbances [at 859 and 853 cm^{-1} (*)] associated with the CS stretch of an N-bonded thiocyanate ligand. The absence of this feature in the lower trace is consistent with the S-bonded structure discussed in the text.

Table II. Summary of the CS Stretching IR Data for M–NCS Complexes[a]

compound	^{12}C ν/cm^{-1}	^{13}C ν/cm^{-1}	^{15}N ν/cm^{-1}
Pt[(bpy)$(NCS)_2$] (II)	859.2, 852.5	849.6 [850.4]	847.7 [850.4]
		843.8 [841.6]	840.9 [843.8]
Pt[(phenan)$(NCS)_2$]	857.3 sh	844.7 sh [846.3]	845.7 [848.6]

[a] The numbers in brackets refer to the values calculated for $^{12}C^{14}N^{32}S$, making the assumptions discussed in the text.

at 2117 cm^{-1} is the dominant feature in the resolved data, but the relative contribution of the other two components (at 2128 and 2108 cm^{-1}) appears to be somewhat variable from sample to sample. The average line width of the latter absorbance, 24.9 cm^{-1}, which is presumed to arise from a near superposition of two absorbances, is significantly broader than that of the other two components. Finally, it is worth noting that the sum of the fractional areas under the two "outside" bands is approximately equal to that under the 2117-cm^{-1} band. These data suggest that there are two distinct sets of pseudohalide ligands present in II, each giving rise to a symmetric and asymmetric CN stretch, with an accidental degeneracy of the symmetric stretch of one pair and the asymmetric stretch of the other giving rise to the most intense band at 2117 cm^{-1}. It is interesting to note that two of these (presumed) four absorbances in II are essentially identical with the two CN stretches observed in I, although in I both thiocyanate ligands are S-bonded. Since the solid-state NMR data of II show that these ligands are N-bonded, a possible explanation for the observed results may involve the existence of both "eclipsed" and "staggered" conformations making up two distinct sets of Pt–Pt chains. The presently available data are not sufficient to rigorously support this hypothesis.

Infrared data below 1000 cm^{-1} have also been examined in detail in this study. The CS stretching mode of metal thiocyanates has been found to be diagnostic of the nature of the pseudohalide bonding.[19] Generally, IR bands in the range $720 < \nu < 680$ cm^{-1} are observed with M–S bonding, while the appearance of these features between 860 and 790 cm^{-1} is associated with M–N bonding, although these generalizations must be applied with some caution.[20] The relevant portions of the IR spectra for compounds I and II are shown in Figure 2. The absence of an observable band, characteristic of ν_{CS} in the spectrum of I, and its presence (at ca. 857 cm^{-1}) in II is in accord with the postulate that I and

(12) Bertini, I.; Sabatini, A. *Inorg. Chem.* **1966**, *5*, 1025.
(13) Burmeister, J. L.; Basolo, F. *Inorg. Chem.* **1964**, *3*, 1587.
(14) Turco, A.; Pecile, C. *Nature* **1961**, *191*, 66.
(15) Preetz, W.; Fricke, H.-H. *Z. Anorg. Allg. Chem.* **1982**, *486*, 49; Basolo, F.; Baddley, W. H.; Burmeister, J. L. *Inorg. Chem.* **1964**, *3*, 1202.
(16) Basolo, F.; Burmeister, J. L.; Weidenbaum, K. J. *J. Am. Chem. Soc.* **1966**, *88*, 1576.
(17) Savoie, R.; Pezolet, M. *Can. J. Chem.* **1967**, *45*, 1677; Rutherford, P. E.; Thornton, D. A. *Spectrosc. Lett.* **1980**, *13*, 427.
(18) Pinchas, S.; Laulicht, I. *Infrared Spectra of Labelled Compounds*; Academic Press: New York, 1971; ^{13}C, pp 201–215; ^{15}N, pp 216–237.
(19) Basolo, F.; Burmeister, J. L.; Poe, A. J. *J. Am. Chem. Soc.* **1963**, *85*, 1700.
(20) Jones, L. H. *J. Chem. Phys.* **1958**, *28*, 1234.

Table III. ^{13}C and ^{15}N NMR Data for the -SCN Ligand

compound Pt[L(SCN)$_2$]	form	^{13}C solution/ppm[a]	^{13}C solid state/ppm[b]	^{15}N solid state/ppm[c]
L = 2,2′-bpy	yellow	114.6	113.0, 116.9[d]	233.6
	red[e]		124.0	62.9[f]
L = 1,10-phen[g]	yellow	114.2		229.1
	red[h]			63.9[i]

[a] Data aquired in NMP, referenced to DMSO-d_6 at 39.4 ppm from TMS. [b] Data referenced to adamantane at 29.1 ppm from TMS. [c] Data referenced to $(^{15}NH_4)_2SO_4$ at 0.00 ppm. [d] Splitting due to solid state sampling effects (see reference 25). [e] Conversion of yellow to red forms by heating of the neat solid or recrystallization from DMSO, see text. [f] $^1J(^{195}Pt-^{15}N)$ = 216.0 and 229.5 Hz. [g] L = phen are included for comparison. [h] The N-bonded phen compound obtained from DMSO exhibited a weak resonance at ~230 ppm from residual Pt-S-CN complex, which is an equilibrium product in solution. [i] $^1J(^{195}Pt-^{15}N)$ = 206.3 and 217.1 Hz.

II involve S- and N-bonded structures, respectively. The inability to identify this mode in the IR spectra of I may be due to a shift of unknown magnitude, a change in the oscillator strength of this mode (making it difficult to identify in a region where numerous ligand absorbances occur), or a combination of these. Complex II exhibits absorbances at 859.2 and 852.5 cm^{-1}, associated with the symmetric and asymmetric modes, as a result of the ligand isomerization to the isothiocyanate form. Isotopic substitution (^{13}C and ^{15}C, separately) of the SCN ligand gave rise to characteristic "red shifts" of the CS bands,[17,18] while the bpy modes remain uneffected. The observed shifts of the labeled species can be related to the frequencies associated with the natural abundance data by assuming that the CN moiety acts as a unit, coupled by harmonic oscillator behavior to the S atom. The observed values, as well as the calculated frequencies, are summarized in Table II. Implied in the foregoing is the assumption that the CS bond order does not change appreciably in the change from M–S to M–N bonding. This assumption is supported by crystal structure data for the Pt–S bonded *trans*-Pt(py)$_2$(SCN)$_2$[21] and the Pt–N bonded Pt(bpym)(NCS)$_2$·NMP (where py = pyridine, bpym = 2,2′-bipyrimidine, and NMP = *N*-methylpyrrolidone),[22,23] which have pseudohalide CN bond lengths of 1.14 and 1.11 Å, respectively.

(b) NMR Data. The ^{13}C and ^{15}N chemical shifts of I and II, under various conditions, are summarized in Table III.

The ^{13}C solution experiments were carried out only on the yellow (S-bonded) form (I) since it was found in this study that the corresponding red (N-bonded) form (II) dissolves with reisomerization to I at (or slightly above) room temperature. Complex I was found to be appreciably soluble in *N*-methylpyrrolidone (NMP), and dilute solutions are stable for several hours at room temperature without precipitation of the red complex. Both the bipyridyl and corresponding phenanthrolyl complexes show a thiocyanate ^{13}C resonance at about 114 ppm, indicative of Pt–S^{13}CN bonding.[24] Splitting is seen in the ^{13}C resonances of the bidentate ligand due to solid-state effects caused by the precipitation of small amounts of the N-bonded polymer during data acquisition. No major chemical shift anomalies associated with the C atoms of the bpy or phenan ligands, compared to the corresponding chloro complexes,[23] were observed, and these data will not be further discussed.

Because of the difficulties, arising from the very limited solubility of the red platinum thiocyanate complexes, involved in obtaining comparison NMR spectra of the two forms, ^{13}C and ^{15}N MAS solid sample NMR was used to further elucidate the molecular level changes associated with the I → II conversion. Initial MAS experiments on the bpy complexes were carried out using ^{13}C-enriched samples. Compound I evidenced a split resonance with components at 113.0 and 116.9 ppm. The centroid of this doublet agrees well with the ^{13}C solution experiments, referred to above, while the observed splitting can be attributed to effects introduced by the solid-state sampling.[25] A single thiocyanate carbon resonance is observed for II, with a chemical shift of 124.0 ppm, indicative of Pt–N^{13}CS bonding. The lack of splitting of this signal is presumably a consequence of the higher degree of ordering associated with "stacking" of the monomers to yield Pt–Pt chains in this complex (vide infra).

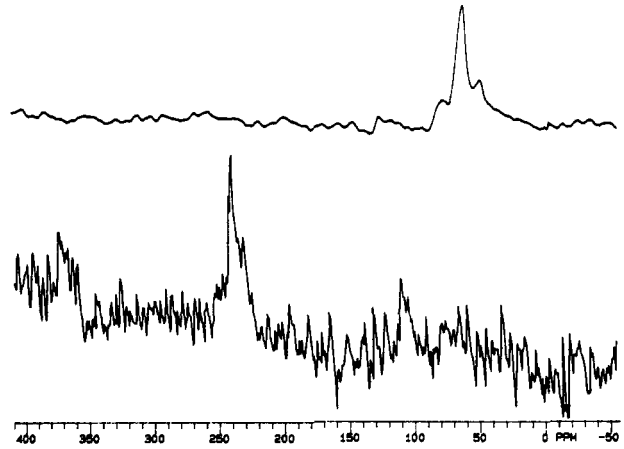

Figure 3. ^{15}N MAS NMR spectra of Pt[(bpy)(NCS)$_2$] (I, top trace, 200-MHz Varian XL) and Pt[(bpy)(SCN)$_2$] (II, bottom trace, 270-MHz JEOL). The two smaller resonances noted in the spectrum of (I) arise from the coupling between ^{195}Pt (s = $^1/_2$) and ^{15}N (s = $^1/_2$).

Although the ^{13}C NMR experiments were suggestive of the Pt–S vs Pt–N transformation, the 10 ppm difference in the chemical shift of the thiocyanate resonances left some room for uncertainty, which was subsequently resolved by ^{15}N MAS experiments on the same sample pair. The advantage of ^{15}N-labeled NMR experiments arises from the much larger chemical shift differences (δ > 200 ppm for Pt–S and δ ~ 60 ppm for Pt–N thiocyanates[26]), thus permitting a much clearer interpretation of the results. NMR data for the ^{15}N-labeled forms of I and II are shown in Figure 3. As summarized in Table III, the ^{15}N resonance appears at 233.6 and 233.0 ppm for the S-bonded bpy and phenan complexes, respectively. The N-bonded complexes evidence nitrogen resonances at 65.1 and 63.8 ppm, respectively. Moreover, both of the latter resonances are accompanied by "satellite bands" arising from the coupling of the ^{15}N (s = $^1/_2$) and ^{195}Pt (s = $^1/_2$) spins, with $^1J(^{195}Pt-^{15}N)$ values of ~225 Hz, in agreement with literature values.[27] These "satellites" are, of course, unobservable in the spectra of the S-bonded isomers as a result of the absence of Pt–S (spin–spin) coupling due to the s = $^3/_2$ of sulfur.

In summary, the solid-state NMR experiments provide unambiguous evidence for ligand isomerization in the I → II transformation in these complexes, consistent with the infrared inferences reported above. Finally, in this context, it is worth noting that scanning gravimetry studies on both I and II have been carried out to a precision of ±0.05%. The loss of one water molecule per complex would entail a weight loss of 3.85%, but no significant loss of weight of the samples in the temperature range 300 < T K < 625 was observed. Hence, the I → II transformation does not involve the loss of solvent (H_2O) from the matrix but is an intrinsic property of the anhydrous complex.

(c) EXAFS Evidence for Ligand Isomerism and Molecular Stacking. The two major questions addressed in the present study, ligand isomerism and the formation of chain polymers involving Pt–Pt stacking, have proven to be susceptible to elucidation by

(21) Caira, M. R.; Nassembeni, L. R. *Acta Crystallogr.* **1975**, *331*, 581.
(22) Cohen, S.; Coyer, M. J.; Herber, R. H., unpublished results.
(23) Coyer, M. J. Ph.D. Thesis, Rutgers University, 1991.
(24) Kargol, J. A.; Crecely, R. W.; Burmeister, J. L. *Inorg. Chem.* **1979**, *18*, 2532.
(25) Stefaniak, L.; Ando, I.; Yoshimizu, H.; Lipkowski, J.; Webb, G. A. *J. Crystallogr. Spectrosc. Res.* **1991**, *21*, 51.
(26) Pregosin, P. S.; Streit, H.; Venanzi, L. M. *Inorg. Chim. Acta* **1980**, *38*, 237.
(27) Appleton, T. G.; Hall, J. R.; Ralph, S. F. *Inorg. Chem.* **1985**, *24*, 4685; Kerrison, D. J.; Sadler, P. J. *J. Chem. Soc., Chem. Commun.* **1977**, 861.

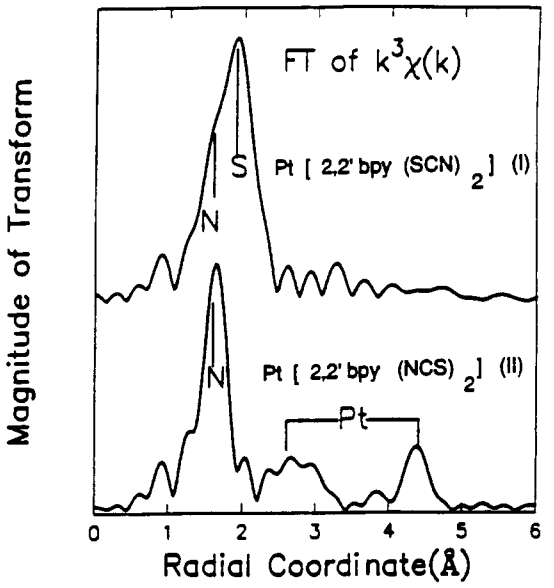

Figure 4. Comparison of the FT's of the room temperature EXAFS results for $k^3\chi(k)$ for I and II. The yellow complex (I) shows evidence for both N and S nearest neighbor (nm) atoms, while the red complex (II) shows only N nn atoms, together with two features identified as arising from Pt–Pt scattering.

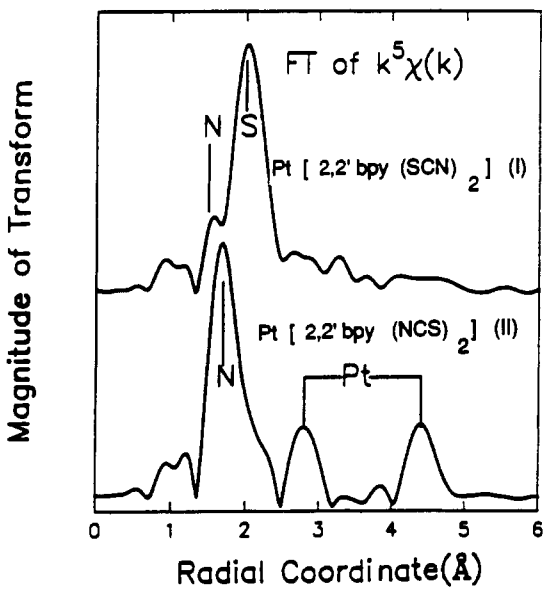

Figure 5. Same as Figure 4, except that the $k^5\chi(k)$ analysis emphasizes the two features identified as due to Pt back-scattering.

Pt EXAFS techniques. A more detailed discussion of the X-ray absorption studies on this class of square planar Pt compounds will appear elsewhere.[28]

In EXAFS analysis the focus is on the normalized wavenumber (k) dependent oscillation of the X-ray absorption coefficient about the average $\chi(k)$.[29,30] The Fourier transform of the weighted function $k^n\chi(k)$ to real space (denoted hereafter as FT) exhibits peaks at positions corresponding to back-scattering maxima from atomic near-neighbor shells. Thus, FT curves convey information similar to a radial distribution function (RDF). However, there are two disparities (from a true RDF) to emphasize. First, the FT peak intensities involve both the atomic back-scattering cross section and the k-weighting factor.[30] Second, the FT peak positions involve an atomic back-scattering phase shift, and hence, the FT peaks occur at distances shifted from the true RDF interatomic separation peaks.[30]

Figure 4 shows the FT of $k^3\chi(k)$ for both the $\{Pt[(bpy)(SCN)_2]\}$ and $\{Pt[(bpy)(NCS)_2]\}$ forms of the two compounds examined in detail in this study. The atoms associated with the various FT features, identified below, are labeled in the figure. It is clearly evident from the EXAFS results that while both S and N are present in the Pt nearest neighbor shell in I, only N is present in the first shell of II. This conclusion follows from the observation that the double maximum feature between 1.3 and 2 Å in the spectrum of the former has collapsed to a single peak (centered at 1.60 Å) in the spectrum of the latter. Thus a ligand flip has occurred in the I → II conversion.

A standard least-squares fitting method has been used to estimate the ligand coordination and bond length in these materials.[29,30] As applied to the N shell in II, for example, this method entails the following: measuring the EXAFS for a known standard, in this case $Pt\{bpy(NCO)_2\}$;[31] determining the back-scattering amplitude and phase shift from this standard's known bond length (1.99 Å) and 4-fold N-coordination; assuming the transferability of these parameters to II; and minimizing the theoretical versus experimental $k^3\chi(k)$ difference with respect to the Pt–N bond length and coordination. This procedure yields a Pt–N bond length in II of 1.97 ± 0.01 Å and an N-coordination of 3.63 ± 0.67. This bond length is close to those reported for structurally similar compounds,[29-31] and, considering the typically large coordination shell uncertainties, the 4-fold coordination is also clear.

The overlapping S and N features in the FT for I (see Figure 4) require a more involved two-shell fitting method. For this analysis, the $n = 2$ weighting of $k^n\chi(k)$ has been used because the S and N FT features have comparable strengths with this lower k-weighting of $\chi(k)$. (It should be noted that the sulfur FT feature increasingly dominates that of the nitrogen related feature as n becomes larger; for comparison, see Figures 4 and 5.) In the two-shell fit, the compound $K_2Pt(SCN)_4$, with a Pt–S distance of 2.29 Å, has been used as a four-coordinate sulfur standard, and $Pt[(bpy)(NCO)_2]$, with a Pt–N distance of 1.99 Å, as a four-coordinate nitrogen standard. From this analysis, the results are 2.66 ± 0.79 sulfur atoms at 2.24 ± 0.02 Å and 1.34 ± 0.79 nitrogens at 1.97 ± 0.02 Å. Within the large coordination uncertainty, these results support the "flip" on both SCN ligands accompanying the yellow to red conversion.

A further point to be noted in Figure 4 is the appearance of two new features (near 2.8 and 4.3 Å) in the FT-EXAFS spectrum of II in a region where the spectrum of I is structureless. In order to determine if these features reflect Pt–Pt interactions, it is helpful to compare the FT of the $k^5\chi(k)$ results for the two forms of the complex. The enhancement of these features (Figure 5) relative to those in the $k^3\chi(k)$ results (Figure 4) indicates their origin in back-scattering from high Z atoms for which $F(k)$, the atomic back-scattering amplitude, is strongly weighted toward high k. Since the only heavy atom in these complexes is the Pt atom, the conclusion that these features reflect metal–metal interactions seems justified.[32]

Further confirmation of the Pt–Pt origin of these features can be obtained from back-transforming (within a real-space window bracketing the feature) the FT of the $k^n\chi(k)$ results to k-space. Thermal disorder is well known to dampen significantly the EXAFS oscillations and reduce the amplitude of the coordination peaks in the FT radial distribution curves.[29,32] This is especially true for high-k related peaks (e.g., Pt–Pt interactions).[33] In order to improve the signal to noise ratio for this analysis, low temperature ($T = 15$ K) EXAFS measurements were performed, and

(28) Coyer, M. J.; Croft, M.; Chen, J.; Herber, R. H. to be published.
(29) Eisenberger, P.; Kincaid, B. M. *Science* **1978**, *20*, 1441; Fan, M. J.; Proctor, A.; Hoffmann, D. P.; Hercules, D. M. *Anal. Chem.* **1988**, *60*, 1225A.
(30) Teo, B.-K.; Kijima, K.; Bau, R. *J. Am. Chem. Soc.* **1978**, *100*, 621.
(31) Coyer, M. J.; Herber, R. H.; Cohen, S. *Inorg. Chim. Acta* **1990**, *175*, 47; *Ibid. Acta Crystallogr.* **1991**, *C47*, 1376.
(32) Hitchcock, A. P.; Lock, C. J. L.; Lippert, B. *Inorg. Chim. Acta* **1986**, *124*, 101.
(33) Teo, B. K. *EXAFS: Basic Principles and Data Analysis*; Springer Verlag: New York, 1986; Teo, B. K.; Lee, P. A.; Eisenberger, P.; Kincaid, B. M. *J. Am. Chem. Soc.* **1977**, *99*, 3854.

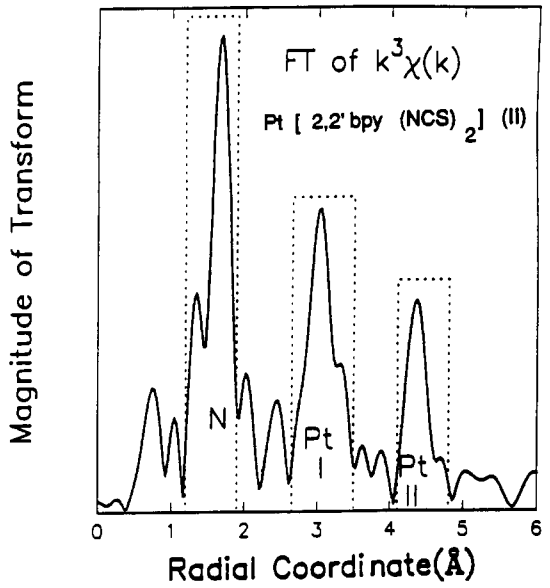

Figure 6. FT of the 15 K EXAFS data for II using $k^3\chi(k)$. The back-transform "windows" for the N, Pt_1, and Pt_2 features are indicated by the dashed lines.

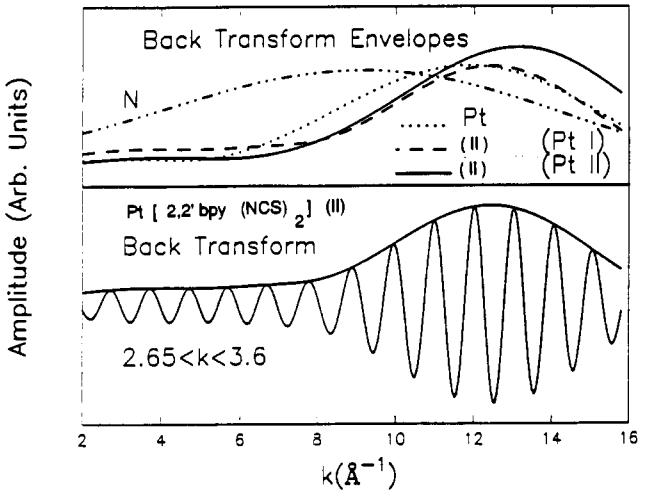

Figure 7. (Bottom) Back-transformed, filtered FT $k^3\chi(k)$ results for II at 15 K in the Pt_1 window of Figure 6. Both the EXAFS oscillations and the amplitude envelope resulting from the back-transform are shown. (Top) Analogous amplitude envelopes for the proposed Pt_1 (solid line) and Pt_2 (dashed line) features for II at 15 K. Again, the indicated back transform windows are as shown in Figure 6. The amplitude envelope for the strongest feature in the reference (elemental) Pt is shown for comparison (dotted line). For contrast, the amplitude envelope for the low-Z N nn feature (see Figure 6 for the appropriate window) is also shown.

the resulting FT results are shown in Figure 6. The dramatic Debye–Waller factor enhancement of the two presumed Pt–Pt features [Pt_1 and Pt_2] is clearly noticeable in a comparison of Figures 5 and 6. The k dependence of the amplitude envelope of the back-transformed data (from the two windows indicated in Figure 6) is shown in Figure 7, along with a similar amplitude obtained from a known[34] Pt–Pt feature in an elemental platinum standard. The sharp rise in amplitude for k above 9 Å^{-1}, with a broad peak in the 10–14-Å^{-1} region, is clear evidence for Pt involvement in the back-scattering process. [The elemental Pt data were taken at room temperature; hence thermal disorder shifts its envelope peak to somewhat lower k.] For comparison, the very different k dependence of the back-transforms of the low Z N-feature is also shown. Thus, analysis clearly identifies two Pt–Pt distances in the spectra of Pt[(bpy)(NCS)$_2$].

Due to the presence of C and N atoms in the ligands which fall in the 3.2–5-Å range, application of the fitting method to the Pt related features is not feasible. Instead, a standard "ratio method" decomposition of the phase component of the EXAFS to estimate the Pt–Pt bond lengths has been employed. This method involves the use of a standard, in the present case the 2.776-Å nearest-neighbor shell of elemental Pt.[34]

Essentially, this method involves assuming that the k-dependent phase shifts of the unknown (here compound II) and a standard (here the nearest-neighbor shell in elemental Pt) are the same and associating the change in the period of the EXAFS oscillation solely with the standard-to-unknown shell radius change. Using this ratio method, the two Pt–Pt distances for II are calculated to be 3.24 ± 0.05 and 4.52 ± 0.02 Å. The former of these distances can be identified with the metal–metal distance in "stacked" Pt(II) complexes,[32,35-37] while the second distance involves a longer interaction. One of the reviewers has pointed out that this longer interaction may arise from a structure in which dimeric units, with Pt–Pt distances of 3.24 Å, form chains with a separation of 4.52 Å between adjacent dimers. Such a structure would, of course, give rise to two distinct scattering maxima in the EXAFS FT. The strength of this larger-distance FT feature indicates that this interaction is fairly robust. The absence of this feature in the spectra of I suggests that in that case the solid consists of independent monomeric units with no significant interunit bridging.[32]

From the above data, it is concluded that the I → II conversion in Pt[(bpy)(SCN)$_2$] involves both ligand isomerization and "stacking" of the monomeric units into a quasilinear array involving Pt–Pt bonding. This polymerization accounts as well for the decreased solubility of II (compared to I) in inocuous solvents. The sequence of these two processes, and the question of whether these two molecular-level events are correlated or independent, cannot be unambiguously answered from the present data.

Acknowledgment. This research was supported in part by the Research Council (M.C.) and by the Research Council and the Busch Fund, Rutgers University (R.H.H.). The infrared spectrometer used in these studies was obtained under Grant 87-0208 from the NIH. We are indebted to Dr. S.-P. Szu for assistance with the solid-state NMR measurements herein reported and to Prof. M. Greenblatt for the use of the thermogravimetric equipment.

(34) Stern, E. A.; Bunker, B. A.; Heald, S. M. *Phys. Rev.* **1980**, *B21*, 5521.
(35) Krogmann, K. *Angew. Chem., Int. Ed. Engl.* **1969**, *8*, 35.
(36) Osborn, R. S.; Rogers, D. *J. Chem. Soc., Dalton Trans.* **1974**, 1002.
(37) Che, C.-M.; He, L.-Y.; Poon, C.-K.; Mak, T. C. W. *Inorg. Chem.* **1989**, *28*, 3081.